# FLUORESCENCE RECOVERY AFTER PHOTOBLEACHING (FRAP) EXPERIMENTS UNDER CONDITIONS OF UNIFORM DISK ILLUMINATION

## Critical Comparison of Analytical Solutions, and a New Mathematical Method for Calculation of Diffusion Coefficient D

ANDRÉ LOPEZ, LAURENCE DUPOU, ANNE ALTIBELLI, JOËL TROTARD, AND JEAN-FRANÇOIS TOCANNE
*Centre de Recherche de Biochimie et Génétique Cellulaires du Centre National de la Recherche Scientifique, 31062 Toulouse Cedex, France*

ABSTRACT A simple fluorescence recovery after photobleaching (FRAP) apparatus using a fluorescence microscope with a conventional mercury arc lamp, working under conditions of "uniform disk illumination" is described. This set-up was designed essentially for the use of anthracene as fluorescent probe, which is bleached (photodimerization reaction) by illumination in the near ultraviolet range (360 nm). It is shown that the lateral diffusion coefficients $D$ can be readily calculated from fluorescence recovery curves using a finite differentiate method in combination with statistical analysis of the data. In contrast to the analytical solutions so far described, this numerical approach is particularly versatile. With a minimization algorithm, $D$ and the probe mobile fraction can be readily calculated for any recovery time under various experimental conditions. These include different probe concentration profiles in the illuminated area after the bleaching step, and situations of infinite or noninfinite reservoir in the diffusion area outside the illuminated area.

### INTRODUCTION

To investigate both the lateral distribution and motion of intrinsic membrane lipids, we have developed a new photochemical technique using anthracene attached to a fatty acid as photoactivatable group (1). This hydrophobic group, which is well suited for labeling the hydrophobic core of the membrane, is fluorescent, but under illumination at 360 nm it forms also 9-9′, 10-10′ covalently bound dimers, which are not fluorescent. Thus, after incorporation into membrane lipids, it can be used to (*a*) evaluate membrane fluidity, (*b*) measure the lateral diffusion rate of the labeled molecules either using a FRAP technique or from the kinetics of the photodimerization reaction, or (*c*) study the topological distribution of lipids in membranes after photo-cross-linking of adjacent anthracene-labeled molecules (dimerization), and subsequently identify the photodimers.

9-(2-Anthryl)-nonanoic acid and various corresponding anthracene-phospholipids have been synthesized (1). Their physical and phase properties have also been investigated (1, 2). A simple and versatile photo-cross-linking method has been described for the determination of the lateral distribution of lipids in model and natural membranes (3). The anthracene-fatty acid has been shown to be incorporated metabolically into the membrane lipids of the bacterium *Micrococcus luteus* (4). The photo-cross-linking method has provided evidence that the lateral distribution of these lipids is homogeneous in the bacterial membrane (5). Extending this method to eukaryotic cells, we have recently shown that 9-(2-anthryl)-nonanoic acid is metabolically incorporated at a high rate into the various membrane glycerophospholipids of Chinese hamster ovary cells (CHO) (6). This has enabled the lateral diffusion rate of intrinsic lipids in living cells to be determined.

Monitoring FRAP experiments with anthracene as a fluorophore requires ultraviolet (UV) irradiation in the range of 340 to 380 nm (1). In this region, a laser as illumination source might represent a practical solution. However, fast bleaching (dimerization) can in fact be readily achieved with a fluorescence microscope, using the intense illumination at 360 nm derived from a conventional mercury arc lamp.

An experimental set-up was constructed in which the size of the illuminated area was determined by a calibrated pinhole interposed in the excitation beam in the conjugated

Address correspondence to Dr. Jean-François Tocanne.

image plane of the microscope. In this configuration, bleaching experiments are operated under conditions of "uniform disk illumination" for which mathematical models are available for calculation of $D$ (7–11).

In addition to a critical evaluation of these various models, we describe the experimental set-up and the mathematical and statistical methods used to analyze the fluorescence recovery data. They are based on the method of finite differentiation.

## MATERIAL AND METHODS

### Chemicals

Synthesis of *sn*-l-acyl-*sn*-2-[9-(2-anthryl)-nonanoyl]-glycerophosphocholine (EAPC) from egg yolk lysolecithin has been described previously (1). Egg yolk phosphatidylcholine (egg-PC) was obtained from Sigma Chemical Co., St. Louis, MO. 5-(*N*-Hexadecanoyl)-aminofluorescein (HEDAF) was purchased from Molecular Probes Inc., Eugene, OR. The purity of these compounds was checked by thin layer chromatography. Solvents were of analytical grade.

### Preparation of Hydrated Egg Phosphatidylcholine Multilayers

EAPC and HEDAF were added to egg-PC at a molar ratio of 1 and 0.5%, respectively. 2 mg of the lipid mixture in chloroform solution were deposited on a microscope slide, and the solvent was evaporated under reduced pressure. Lipids were hydrated by immersing the plate in distilled water for 10 min at room temperature.

Large domains of multilayers were obtained by pressing the hydrated lipids between the slide and a coverslip at a pressure of 60 N/cm$^2$ (12). The preparation was then sealed with paraffin wax to prevent dehydration and stored at 4°C under an atmosphere of nitrogen saturated with water vapor.

### FRAP Apparatus and Experiments

FRAP experiments were carried out using an epifluorescence microscope (Leitz, Ortholux II, Wetzlar, FRG) equipped with a conventional mercury arc lamp (Osram, Munich, FRG, HBO 100 W/2), and the usual combination of dichroic mirror and optical filters for separation of the fluorescence from the excitation beam. The size of the excitation spot was determined by means of calibrated pinholes placed in the excitation beam, in the conjugated image plane. The duration of illumination was controlled by a fast electronic shutter. Fluorescence intensity was measured with a highly sensitive photomultiplier (EMI Electron Tubes Ltd., Ruislip, England, 9558 B) connected to an amplifier. A field diaphragm (calibrated pinhole) was also interposed in the emission beam, just in front of the photomultiplier tube in the conjugated image plane, to select the fluorescence signal originating from the illuminated area (13, 14). The FRAP experiments were monitored using a dedicated Apple II E microcomputer which was also employed for the rapid acquisition, storage, and pretreatment of the fluorescence data. The absolute experimental error in determining the fractional fluorescence recovery rates was estimated to be <0.02. The lateral diffusion coefficients $D$ were calculated using a microcomputer (Wang VP 2000 or Normerel OP AT).

The calibrated pinholes ensured the condition of "uniform disk illumination." However, Fig. 1 *b* shows that this condition was not completely achieved. A slightly trapezoidal beam profile was observed. This diagram corresponds to the optical density profile of a micrograph of an illuminated area obtained, for given pinhole and objective, by focusing within a thin layer of a 5-mM methanolic solution of fluorescein between the slide and the coverslip. Due to the rapid diffusion of fluorescein in the bulk solution, it was assumed that at any point of the illuminated area the fluorescence signal was proportional to the intensity of the incident light. This type of profile was recorded for various pairs of pinhole and objective. Measurement of their width at half-height gave the diameter 2 $ri$ of the corresponding illuminated area (Fig. 1 *b*). All these experiments were carried out under nonsaturating conditions of illumination with respect to both the sample and the film negative.

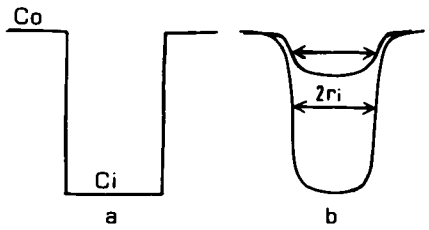


FIGURE 1 Light intensity profiles in the illuminated area. (*a*) Square-well profile corresponding to the theoretical condition of "uniform disk illumination." *Ci* and *Co* indicate respectively the fluorophore concentrations inside and outside the illuminated area after the bleaching step. (*b*) Experimental trapezoidal profiles observed after densitometric scanning of micrographs of the illuminated area (see Material and Methods). These diagrams were obtained for two exposure times and under unsaturating conditions of illumination. In each case, the horizontal bar indicates the diameter 2 $ri$ of the illuminated area measured at half-height of the well.

FRAP experiments were achieved under conditions of constant incident light intensity (Fig. 2). First, the fluorescence intensity was recorded for a limited duration of photobleaching. This allowed us to control the extent of photobleaching, and to determine its kinetic order. Fluorescence recovery was then monitored stepwise (seven steps) by repeating measurements of the fluorescence intensity over short intervals (5 ms) after regular periods in the dark.

To produce reliable results, FRAP experiments must satisfy certain conditions related to the laws of diffusion. For a given fluorophore and for

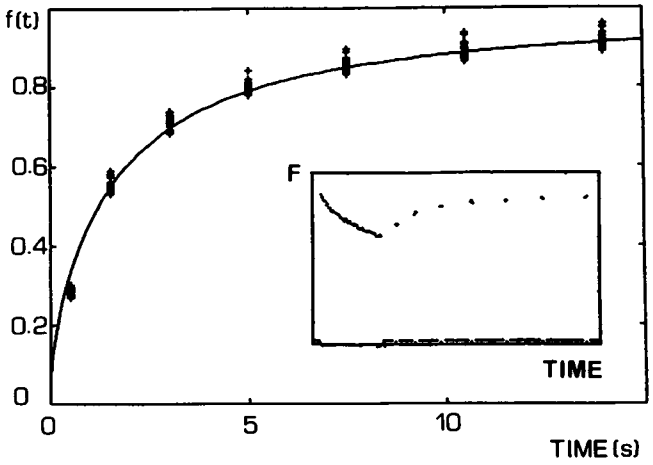


FIGURE 2 Experimental and calculated fractional recovered fluorescence intensities with time. Data (+) shown in this figure refer to a set of FRAP experiments (25 experiments) carried out with EAPC inserted at a concentration of 1% in egg-phosphatidylcholine multilayers. The radius $ri$ of the illuminated area was 4.2 μm. The full line (—) is the best recovery curve which could be calculated using the finite differentiate method. It accounts for a lateral diffusion coefficient $D = 3.53 \pm 0.02\ 10^{-8}$ cm$^2$/s (see Table I). The insert illustrates one typical FRAP experiment with the recording of the bleaching step and of seven fluorescence recovery values. Time axis = 464 ms for the bleaching step; 14 s for the recovery step (see Material and Methods).

given values of the radius *ri* of the illuminated area and the lateral diffusion coefficient *D*, the duration of bleaching must not exceed 5% of the fluorescence recovery half-time (15). The radius of the illuminated area must be small (<25% for $D = 10^{-9}$ cm$^2$/s) with respect to the radius of the diffusion area (conditions of infinite reservoir). The extent of bleaching, which is time-dependent, must be sufficient for accurate determination of the fluorescence recovery (signal/noise ratio). Nevertheless, bleaching cannot exceed a certain rate and time, above which the initial condition of square-well probe concentration profile will no longer be satisfied due to too large a flux of bleached and unbleached particles between the illuminated and diffusion area, at the boundary of the illuminated area.

For egg-PC multilayers and under our conditions, HEDAF and EAPC photobleaching rates of ~30–40% were regularly observed with a Leitz ×63/1.3 oil immersion objective for a duration of illumination of 464 ms. Accurate measurement of *D* can be obtained with such bleaching rates. For diffusion coefficients around $10^{-8}$ cm$^2$/s, which are usually found in model lipid membranes (12, 16), a bleaching time of 464 ms imposes a rather large diameter for the illuminated area. A radius *ri* of 4.2 μm was chosen, which is quite compatible with the size (~100 μm) of the uniform lipid bilayer domains which are usually found in lipid multilayers. Under these conditions, the half-time of fluorescence recovery was found to be ~5 s, which was sufficiently long compared with the bleaching time.

The strong illumination used could have induced a local increase in temperature during the bleaching period. This might have increased the lateral mobility of lipids (12, 16). In control experiments carried out using fluorescein as a pH indicator, we measured the temperature-induced pH change of a Tris-buffer solution around its pK (7.5). Under our experimental conditions, an illumination time of 464 ms was found to lead to a temperature increase of <0.4 K. This slight increase was not thought to affect significantly the measurement of *D* (12, 16).

## RESULTS AND DISCUSSION

### FRAP Theory

All the mathematical methods for calculation of the lateral diffusion coefficient *D* of a fluorescent probe from fluorescence recovery data are based on the diffusion equation:

$$\frac{\partial C}{\partial t}(r, t) = D\,\Delta C(r, t), \tag{1}$$

and all assume the same boundary conditions:

(*a*) The fluorescent probes are considered to be initially distributed uniformly in an infinite, flat membrane, with an initial concentration *Co* corresponding to an initial fluorescence signal *Fo*.

(*b*) Intense illumination is used to reduce the bleaching time as much as possible. This limits effects of diffusion of molecules between the illuminated and nonilluminated areas. At the end of the photobleaching step, this produces the square-well profile condition for probe concentration (Fig. 1 *a*), leading to uniform fluorescence intensities inside (*Fi*) and outside (*Fo*) the bleached area.

At the end of the bleaching step, the system is then left standing in the dark. Due to the progressive replenishment of the bleached area by new fluorescent probes diffusing in from the infinite reservoir outside, a new fluorescence signal $F(t) > Fi$ can be measured after a finite time *t*, on further illumination of the membrane. For freely diffusing particles, complete fluorescence recovery will be observed for infinite time:

$$F(t) \to Fo \quad \text{for} \quad t \to \infty.$$

For practical and analytical purposes (elimination of the fluorescence background signal), it is more convenient to analyze the fluorescence recovery process in terms of fractional recovered fluorescence intensities $f(t)$:

$$f(t) = \frac{F(t) - Fi}{Fo - Fi}.$$

Elson and Magde (7) and Axelrod et al. (8) were the first to describe an analytical solution in the form:

$$f(t) = 1 - \frac{\tau_D}{t} e^{-2\tau_D/t}\left[I_0\left(\frac{2\tau_D}{t}\right) + I_2\left(\frac{2\tau_D}{t}\right)\right] - 2\sum_{k=0}^{\infty} \frac{(-1)^k(2k+2)!(k+1)!(\tau_D/t)^{k+2}}{(k!)^2((k+2)!)^2}. \tag{2}$$

In this equation, $I_0$ and $I_2$ are modified Bessel functions, $\tau_D = r_i^2/4D$ is the characteristic diffusion time, *ri* the radius of the bleached area, and *D* the lateral diffusion coefficient.

Note that this equation, which was correctly written in Elson's paper, was misquoted in the paper of Axelrod which has been subsequently cited frequently. This equation is unfortunately not convergent for $t/\tau_D \to 0$, because the third term becomes undeterminate. Furthermore, for $t/\tau_D < 0.3$, a considerable computational problem is encountered because in the third term factorial terms must be calculated which rapidly increase from 40 for $t/\tau_D = 0.3$ up to 122 for $t/\tau_D = 0.1$. This effectively restricts the use of the analytical method to $t/\tau_D$ values >0.3. The corresponding recovery curve is shown in Fig. 3 (curve 1, $t/\tau_D > 0.3$). For low values of $t/\tau_D$, asymptotic derivations of this equation are not obtainable.

Using a similar theoretical approach but a somewhat different mathematical derivation, Soumpasis (9) obtained a simpler but equivalent relationship. This extended the calculation of *D* down to $t/\tau_D$ values of 0.05:

$$f(t) = e^{-2\tau_D/t}\left[I_0\left(\frac{2\tau_D}{t}\right) + I_1\left(\frac{2\tau_D}{t}\right)\right], \tag{3}$$

where $I_0$ and $I_1$ are modified Bessel functions.

This equation can be used to calculate a recovery curve that can be superimposed on curve 1 in Fig. 3, for $t/\tau_D > 0.03$.

As pointed out by the author, an asymptotic expansion of the modified Bessel functions can be used for $0 < t/\tau_D < 0.03$.

$$f(t) = \left(\frac{1}{4\pi\tau_D}\right)^{1/2}\left[2 - \frac{1}{2}\left(\frac{t}{4\tau_D}\right) - \frac{3}{16}\left(\frac{t}{4\tau_D}\right)^2 - \frac{15}{64}\left(\frac{t}{4\tau_D}\right)^3 - \cdots\right]. \tag{4}$$

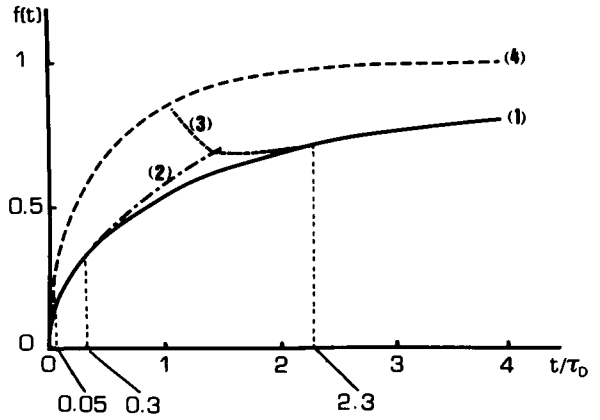


FIGURE 3 Fractional fluorescence intensity $f(t)$ vs. $t/\tau_D$ recovery curves derived from various equations. (*Curve 1*) Finite differentiate method, valid for $t/\tau_D$ varying from 0 to infinite; Eq. 2, valid for $t/\tau_D > 0.3$; Eq. 3, valid for $t/\tau_D > 0.03$; Eq. 4, valid for $0 < t/\tau_D < 0.03$. (*Curve 2*) Eq. 6, valid for $0 < t/\tau_D < 0.05$. (*Curve 3*) Eq. 7, valid for $t/\tau_D > 2.3$. (*Curve 4*) Eq. 8, valid for $t/\tau_D$ varying from 0 to infinite. $\tau_D = r_i^2/4D$ is the characteristic time.

This expression leads to a recovery curve that is superimposable on curve 1 in Fig. 3. It is also in continuity with the curves plotted using Eqs. 2 (curve 1, $t/\tau_D > 0.3$) or 3 (curve 1, $t/\tau_D > 0.03$).

Furthermore, for $t/\tau_D \gg 1$, Soumpasis proposed another asymptotic expansion in the form:

$$f(t) = 1 - \frac{\tau_D}{t} + \left(\frac{\tau_D}{t}\right)^2 - \cdots \quad (5)$$

Here again, the corresponding calculated recovery curve is superimposable on curve 1 in Fig. 3.

Using a different set of theoretical concepts, Lardner (10) proposed two equations covering the two different time domains illustrated by curves 2 and 3 in Fig. 3.

$$f(t) = \frac{1}{\sqrt{\pi}}\left(\frac{t}{\tau_D}\right)^{1/2} \quad \text{for} \quad \frac{t}{\tau_D} < 0.03 \quad (6)$$

$$f(t) = 1 - \frac{\tau_D}{t} + \left(\frac{\tau_D}{t}\right)^2 - \cdots \quad \text{for} \quad \frac{t}{\tau_D} \gg 1. \quad (7)$$

Within their respective time domains, curve 2 ($0 < t/\tau_D < 0.05$) and curve 3 ($2.3 < t/\tau_D$) can be superimposed on curve 1.

It should be noted that Eqs. 4 and 6 are equivalent, and that Eq. 6 can be readily deduced from Eq. 3 using an asymptotic expansion.

Teissié et al. (11) have also proposed a model based on the theory of heat diffusion.

$$f(t) = 1 - 4\sum_{n=1}^{\infty} \frac{e^{-\alpha_n^2 Dt/r^2}}{\alpha_n^2}, \quad (8)$$

in which $\alpha_n$ are the roots of the Bessel function of first kind and order 0.

With the sum extended to $n = 8$, this equation gives the recovery curve 4 in Fig. 3 which is quite different from curve 1. This difference does not stem from the theory of diffusion used to derive Eq. 8, but rather originates from one of the boundary conditions that considers the fluorophore concentration outside the bleached area to be uniform over space and time.

$$C(r, t) = Co \quad r > ri, t > 0.$$

This condition would in fact correspond to production of new fluorophore molecules during the fluorescence recovery process, and is therefore not realistic.

The numerical approach to be described, with the above mentioned boundary condition, yields a recovery curve that can be superimposed on curve 4 in Fig. 3.

Eqs. 2–7 have a formal unity, and within their range of validity, they produce recovery curves which are both similar and in continuity with each other. In principle, judicious combination of these equations should enable $D$ to be calculated for any recovery time. A combination of Eqs. 3 and 6 has been successfully employed to calculate the lateral diffusion coefficient of lipids in embryonic cells (17).

## Calculation of D Using the Finite Differentiate Method

It should be emphasized that all these methods depend on the restricted initial conditions of a square-well concentration profile, and of a membrane that is both flat and infinite. The first condition is not in fact achieved. As shown in Fig. 1 *b*, densitometric scanning of a photograph of an illuminated area revealed a slightly trapezoidal profile of light intensity. Furthermore, in living cells, the condition of infinite reservoir is not necessarily satisfied. This prompted us to reconsider the method for analyzing fluorescence recovery curves. We developed a numerical method based on the scheme of finite differentiate which is described in more detail in Appendix A. This method has the advantage of versatility. It can be used for any conditions of illumination, beam profile, and relative dimensions of bleached and diffusion areas. The distribution of the bleached fluorophore both inside and outside the illuminated area can be calculated at any given time.

## Statistical Analysis of Experimental Data

The lateral diffusion coefficient $D$ of a fluorescent probe can be used to evaluate the dynamic state of the host membrane. Unique values of $D$ are not necessarily found in a given cell population. $D$ can vary with morphological changes, such as the different stages of the cell cycle (18). Furthermore, in living cells, there is the insurmountable problem of cell movement which leads to dispersion of the recovery data. The determination of $D$ therefore needs to

be based on statistical analysis of results from a large number of experiments. Average values of $D$ derived from just the half-recovery times (8) are not adequate. There is a loss of information (not the whole recovery curve), and because $D$ is an explicit parameter, any statistical analysis must rest on the experimental data to be valid (in the present case, on the recovered fluorescence intensities).

In the following discussion (see Appendix B), the lateral diffusion coefficient *Dsol* was evaluated in an iterative way using a minimization algorithm as described by Powell (19) and Lopez et al. (20). This does not require an explicit equation. The value of $D$ corresponding to the best fit with the experimental data, *Dsol*, is simply obtained using the criterion of a minimum sum of the quadratic deviations:

$$S_D^2 = \sum_{i=1}^{N} (f(t_i)_{exp} - f(t_i)_{cal})^2$$

In this equation, $N$ is the total number of experimental recoveries obtained from one set of experiments and used for the computation of $D$ (for example, $N = 7 \times 25 = 175$, in Fig. 2). For the method of finite differentiate, $f(t_i)$ is obtained by interpolation on the recovery curve shown in Fig. 3 (curve 1), which is generated in steps as a function of time.

At the end of the minimization process, the value of the standard deviation $\sigma$, for a set of experiments, is compared to the experimental error: $\Delta f(t_i)$:

$$\sigma = [S_{Dsol}^2/(N - 1)]^{1/2}$$

From a strict statistical point of view, $\sigma$ must be at a minimum and close to the experimental error. If this is the case, the corresponding $D$ value can be considered as the solution *Dsol*. A significant difference between these two values is indicative of a mismatch between the experimental data and the mathematical model used for the analysis.

## Lateral Diffusion Coefficient of HEDAF and EAPC in Phosphatidylcholine Multilayers in an Infinite Reservoir

Egg-phosphatidylcholine multilayers labeled with these two fluorescent probes were investigated in FRAP experiments as described in Material and Methods. At least 20 determinations were carried out on each sample, and the recorded fluorescence recovery values were then subjected to statistical analysis. The calculated diffusion coefficients using either analytical solutions (combination of Eqs. 3 and 6) or the finite differentiate method are shown in Table I. For each probe and for an infinite reservoir (the radius of the diffusion area $R$ was large compared to the radius $ri$ of the illuminated area, $R > 5\ ri$, see Appendix A), similar values of $D$ were obtained with both methods. They were close to the values reported for similar systems (12, 16). Nevertheless, in both cases, a smaller standard deviation $\sigma$ was obtained with the numerical than with the analytical method. In the former, the standard deviation was very close to the experimental error (0.02). For each probe, the mobile fraction was found to be 100 ± 2%. It should be noted that for the numerical approach, a slightly trapezoidal beam profile, as in Fig. 1 *b*, was used (see Appendix A). Small changes in this beam profile had little effect on the calculated values of $D$. The $D_{min}$ and $D_{max}$ values given in Table I correspond to a 95% confidence level. As can be seen in Fig. 4, a 99% confidence level would only slightly enlarge the domain of definition of $D$. It can be seen from Fig. 4 that even with an error risk of 1%, the $D$ values determined for EAPC and HEDAF are statistically different.

TABLE I
LATERAL DIFFUSION COEFFICIENTS $D$ ($10^{-8}$ cm$^2$/s) OF EAPC AND HEDAF IN EGG-PHOSPHATIDYLCHOLINE MULTILAYERS

| Probe used | Numerical solution | Analytical solution, Eqs. 3 and 6 |
|---|---|---|
| EAPC | $3.53 \begin{cases} 3.55 \\ 3.51 \end{cases}$ | $3.31 \begin{cases} 3.40 \\ 3.25 \end{cases}$ |
| | $\sigma = 0.023$ | $\sigma = 0.025$ |
| HEDAF | $3.65 \begin{cases} 3.71 \\ 3.62 \end{cases}$ | $3.40 \begin{cases} 3.48 \\ 3.35 \end{cases}$ |
| | $\sigma = 0.021$ | $\sigma = 0.022$ |

$D_{min}$ and $D_{max}$ are given with 95% confidence level. For each probe, the mobile fraction was found to be 100 ± 2%.

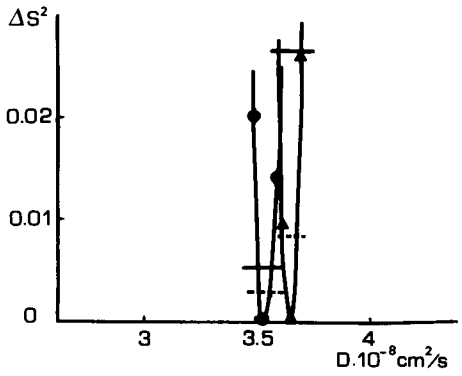


FIGURE 4 Plot of the normalized sum $\Delta S_{Dj}^2 = S_{Dj}^2 - S_{Dsol}^2$ as a function of the lateral diffusion coefficient $D$ for EAPC (●) and for HEDAF (▲) inserted in egg-phosphatidylcholine multilayers. In this expression, $S_{Dj}^2$ and $S_{Dsol}^2$ are defined as being the sum of the quadratic deviations between the observed fluorescence recovery values and the calculated ones, respectively, for a given value $Dj$ of the lateral diffusion coefficient $D$ and the solution value *Dsol*. From these curves and after each *Dsol* was determined using the minimization algorithm, the corresponding minimum ($D_{min}$) and maximum ($D_{max}$) values of *Dsol* were determined for various confidence levels from Snedecor-Fisher's law. In this figure, the horizontal lines give $D_{min}$ and $D_{max}$ for confidence levels of 95% (----) and 99% (—).

## Measurement of the Lateral Diffusion Coefficient of EAPC in Phosphatidylcholine Multilayers in a Noninfinite Reservoir

For particles free to diffuse over a large area compared with the illuminated area (condition of infinite reservoir), complete fluorescence recovery will be obtained if the observation time is long enough. Nevertheless, incomplete recovery may be due either to an immobilized fraction of the bleached particles, or to the fact that the reservoir is noninfinite. These two situations can be discriminated using the numerical method described here. Curve 1 in Fig. 5 shows a calculated recovery curve for a 100% mobile fraction and infinite reservoir. The parameters used for this computation were radius $ri = 2$ μm and $R = 10$ μm for the illuminated and diffusion area, respectively, and a lateral diffusion coefficient $D = 2.10^{-9}$ cm²/s. Curve 2 in Fig. 5 is the same as above, except that the radius of the diffusion area was reduced to only twice that of the illuminated area ($R = 4$ μm). As illustrated by scheme *A* in Fig. 6, conditions of infinite reservoir no longer apply. At the beginning of the recovery process, curves 1 and 2 in Fig. 5 are superimposable, but as soon as the bleached particles reach the limit of the diffusion area (in this case, after ~7 s), the two curves diverge. At the end of the recovery process, the probe concentration in the illuminated area is not *Co* but $C_\infty < Co$. Because the recovery process is expressed in the form of a normalized function, the unrecovered fraction will be directly proportional to the ratio of the surface areas of the illuminated to the diffusion zones. In the present case, with a ratio = ¼ ($R = 2\ ri$), incomplete recovery leads to the appearance of an "immobile" fraction of 25%.

Curve 3 in Fig. 5 and scheme *B* in Fig. 6 illustrate the case of an immobile fraction of 25% with an infinite reservoir ($R = 5\ ri$). Curves 2 and 3 are quite different. It can be seen, therefore, that the numerical method used to simulate these two recovery curves could also be employed to discriminate between the two situations of noninfinite reservoir and potential immobile fraction.

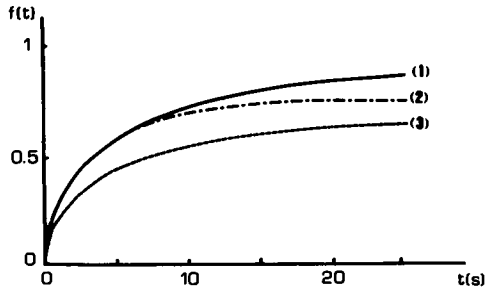


FIGURE 5 Calculated fluorescence recovery curves for various conditions of mobile fraction and radius *ri* and *R* of the illuminated and diffusion area. (*1*) 100% mobile fraction and infinite reservoir, $R = 5\ ri$. (*2*) 100% mobile fraction and noninfinite reservoir, $R = 2\ ri$. (*3*) 75% mobile fraction and infinite reservoir, $R = 5\ ri$. Parameters used: $ri = 2$ mm; $D = 2.10^{-9}$ cm²/s. The probe redistributions in the illuminated area corresponding to curves 2 and 3 are illustrated by schemes *A* and *B* in Fig. 6.

As an experimental verification, FRAP experiments were carried out using EAPC embedded in small egg-phosphatidylcholine multilayers. According to Wu et al. (12), the homogeneous domains observed under the microscope can be considered stacked and flattened liposomes of finite size. Experiments were performed with an illuminated area of radius $ri = 8.75$ μm. The radius of the homogeneous area was chosen to be about twice that of the illuminated area. As expected, the observed fluorescence recovery curves were similar to curve 2 in Fig. 5 with a final recovery around 75% (curves not shown). Double fitting of the data, with respect to *D* and *R*, lead to the following results. The calculated value of *D* varied between 2.4 and 2.8 $10^{-8}$ cm²/s from one experiment to another. They were slightly lower than the value of 3.53 $10^{-8}$ cm²/s determined under conditions of infinite reservoir for large lipid domains. Some dispersion was also observed in the calculated values for *R*: 15–18 μm. However, as expected, these values were about twice the radius $ri = 8.75$ μm of the illuminated area. The standard deviation $\sigma = 0.023$ was similar to that found in large lipid domains under conditions of infinite reservoir (Table I).

Calculation of *D* without taking the limited size of the diffusion area into account lead, on average, to calculated *D* values of ~2.2 $10^{-8}$ cm²/s, with a larger standard deviation $\sigma = 0.055$. A standard deviation nearly threefold higher than the experimental error (0.02) is an indication of the lack of validity of the model used to account for the experimental data.

## CONCLUSION

As mentioned above, derivation of analytical equations for the calculation of *D* under conditions of "uniform disk illumination" is not straightforward. None of the solutions so far reported (7–11) are fully satisfactory, and to account for an entire fluorescence recovery curve they have to be used in combination with each other. Furthermore, these equations are only valid for well-defined experimental conditions of photobleached fluorophore concentration profile in the illuminated area (square-well concentration profile) and of relative size of bleached and diffusion area (infinite reservoir). The numerical method described here can solve many, if not all, of these problems. Ten years ago, routine use of such a method might have presented problems. These obstacles can be readily surmounted with the now quasi-universal laboratory microcomputer. Typically, with this method, one complete minimization process, including the determination of minimum and maximum values, takes ~1 min for one parameter (*D*), 90 min for two parameters (*D* and the mobile fraction *M*) and 4 h for three parameters (*D*, *M*, and *R*, the radius of the diffusion area). In combination with statistical analysis of the data, the finite differentiate method can be used to analyze FRAP data, under a wide range of experimental condi-

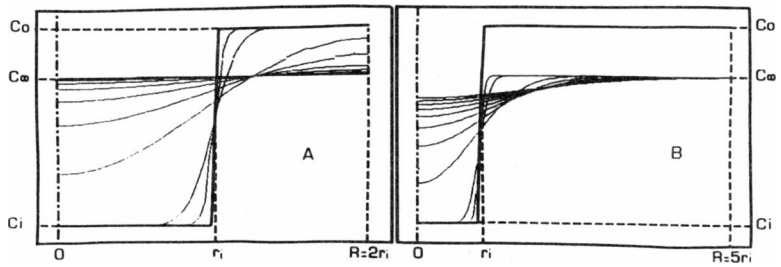


FIGURE 6 Probe concentration profiles during a fluorescence recovery process for various conditions of mobile fraction and radius *ri* and *R* of the illuminated and diffusion area. Scheme *A* refers to conditions of noninfinite reservoir ($R = 2\,ri$) and 100% mobile fraction, and scheme *B* to condition of infinite reservoir ($R = 5\,ri$) and 75% mobile fraction. The thick curves delineate the trapezoidal probe concentration profile obtained after the bleaching step. *Ci* and *Co* are the probe concentrations inside and outside the illuminated area, respectively. The thin lines are the computer-calculated probe concentration profiles after time steps 1, 2 then 100, 200 . . . of the recovery process. Time step was 50 ms. $C_\infty$ is the final probe concentration in the diffusion area after an infinite recovery time. These two schemes correspond respectively to the recovery curves 2 and 3 in Fig. 5.

tions. Its versatility is illustrated by the calculation of *D* under conditions of noninfinite reservoir. This numerical approach could also be used to describe other aspects of membrane dynamics, such as flow processes, which may also disturb diffusional recovery.

## APPENDIX A

## Generation of Fluorescence Recovery Curves Using the Finite Differentiate Method

In the membrane plane, changes in local concentration of a given particle with time due to a diffusional process is given by the diffusion equation:

$$\frac{\partial C(r,t)}{\partial t} = D\Delta C(r,t), \tag{1}$$

where *D* is the lateral diffusion coefficient of the diffusing particle and $\Delta$ is the Laplacian operator.

Due to the axial symmetry in the membrane plane, this diffusion law is better described using cylindrical coordinates.

$$\frac{\partial C(r,t)}{\partial t} = D\left(\frac{\partial^2 C(r,t)}{\partial r^2} + \frac{1}{r}\frac{\partial C(r,t)}{\partial r}\right). \tag{9}$$

$C = C(r,t)$ is the surface concentration of the diffusing species at a distance *r* from the origin (illuminated area center) and at time *t*.

Under conditions of "uniform disk illumination" and at time zero, i.e., at the end of the bleaching step and at the onset of fluorescence recovery, the boundary conditions of probe concentration inside and outside an illuminated area of radius *ri* (Fig. 1) are:

$$C(r,0) = Ci \quad \text{for} \quad 0 < r < ri$$
$$C(r,0) = Co \quad \text{for} \quad r > ri.$$

It should be noted that the finite differentiate method (21) cannot account for a strictly square-well profile of probe concentration, because it is not possible to have two different ordinates (*Ci* and *Co*) for the same abcissa *ri*. The simplest way to overcome this difficulty is to introduce a trapezoidal concentration profile, using the following conditions:

$$C(ri - h, 0) = Ci$$
$$C(ri, 0) = (Co - Ci)/2$$
$$C(ri + h, 0) = Co,$$

where *Ci* and *Co* are the probe concentrations inside and oustide the bleached area, respectively, and *h* is the space-step to be used.

These conditions, which satisfy the continuity of the function, also have the advantage of taking into account the slightly trapezoidal experimental probe concentration profile which is assumed to originate from the slightly trapezoidal light intensity profile shown in Fig. 1 *b*. It should be stressed that within the framework of the finite differentiate method, it is possible to account for any probe concentration profile in the bleached area.

With respect to the diffusion area, two conditions have to be considered, that of infinite reservoir and that of finite reservoir. The condition of infinite reservoir is usually expressed as

$$C(R,t) = Co \quad \text{for} \quad t \to \infty,$$

where *R* is the radius of the diffusion area. This condition, which implies that $R = \infty$ is in fact never encountered experimentally and is therefore unrealistic. It is more realistic to consider a finite reservoir of radius *R* and to apply the boundary condition

$$C(R,t) = C(R - h, t - k) \quad \text{for} \quad t > 0,$$

where *k* is the time-step used.

This condition has the advantage of being general and valid for any value of *D*, *ri*, *R*, and time of observation, *t*. It is referred to here as the condition of finite reservoir and was systematically used in our calculation reported. It is worth emphasizing that the concept of finite or infinite reservoir is relative and depends on the values of *D*, the ratio $R/ri$, and the time of observation *t*. For example, for $D = 10^{-8}$ cm$^2$/s and $t = 20$ s, a ratio $R/ri > 3.5$ will already correspond to the condition of infinite reservoir.

In addition to the spatial discretization (Newton method), a time discretization may be introduced (Crank-Nicholson scheme) (22) and the time integration can be performed numerically. Thus, for *k* and *h* as the time and space steps, respectively, we have:

$$\frac{\partial C(r,t)}{\partial t} = \frac{C(r,t+k) - C(r,t)}{k} \tag{10}$$

$$\frac{\partial C(r,t)}{\partial r} = \frac{1}{4}\left(\frac{C(r+h,t) - C(r-h,t)}{h} + \frac{C(r+h,t+k) - C(r-h,t+k)}{h}\right) \tag{11}$$

$$\frac{\partial^2 C(r,t)}{\partial r^2} = \frac{1}{2}\left(\frac{C(r+h,t) - 2C(r,t) + C(r-h,t)}{h^2} + \frac{C(r+h,t+k) - 2C(r,t+k) + C(r-h,t+k)}{h^2}\right). \tag{12}$$

By combining Eqs. 9–12, it is possible to evaluate this diffusional problem by a scheme of finite differentiation, starting from the space step at the boundary *R* of the diffusion area (Vide supra). For convergence of

the corresponding mathematical linear equations, the values of the time and space step are chosen such that:

$$1 - \frac{Dk}{2h^2} \geq 0$$

Assuming that the fluorescence signal is proportional to the probe concentration, a fluorescence recovery curve can be generated for any definite system: $D$, $ri$, $R$, $k$, $h$.

## APPENDIX B

## Fitting of the Experimental Data

For a given set of experimental fluorescence recovery data, the lateral diffusion coefficient $D$ is calculated using a minimization algorithm. This generates a fluorescence recovery curve for a given value $Dj$ of the lateral diffusion coefficient, which is then compared with the experimental curve. The sum $S^2_{Dj}$ of the quadratic deviations between the calculated and observed recovery values is then calculated. The solution $Dsol$ is obtained when this sum $S^2_{Dsol}$ is at a minimum.

Plotting the dispersion of these sums as

$$\Delta S^2_{Dj} = S^2_{Dj} - S^2_{Dsol}$$

leads to a parabolic curve which has a minimum for $Dj = Dsol$ (Fig. 4).

From this curve, the corresponding minimum ($D_{min}$) and maximum ($D_{max}$) of $Dsol$ can be determined for various confidence levels using Snedecor-Fisher's law (Handbook of Chemistry and Physics):

$$f(\alpha, a, b) = \frac{(S^2_{Dj} - S^2_{Dsol})}{S^2_{Dsol}} \cdot \frac{b}{a}.$$

$f(\alpha, a, b)$ is a coefficient found in tables, which depends on $\alpha$, the degree of uncertainty and $a$ and $b$, the degrees of freedom of the numerator and denominator, respectively.

For a given degree of uncertainty $\alpha$, one can calculate

$$\Delta S^2_{Dj} = \frac{a}{b} \cdot f(\alpha, a, b) \cdot S^2_{Dsol}.$$

The points of intersection with the parabolic curve give the extreme values of $Dsol$, i.e., $D_{min}$ and $D_{max}$.

We would like to thank Dr. J. Teissié for fruitful discussions, and Dr. S. Jarman for rereading the English manuscript.

This work was supported by grants from the Univerité Paul Sabatier (Toulouse), from the Fondation pour la Recherche Médicale, and from the Pole Régional de Génie Biologique et Médical de Toulouse.

*Received for publication 10 August 1987 and in final form 15 February 1988.*

## REFERENCES

1. de Bony, J., and J. F. Tocanne. 1983. Synthesis and physical properties of phosphatidylcholine labelled with 9-(2-anthryl)-nonanoic acid, a new fluorescent probe. *Chem. Phys. Lipids.* 32:105–121.
2. Vincent, M., J. Gallay, J. de Bony, and J. F. Tocanne. 1985. Steady-state and time resolved fluorescence anisotropy study of phospholipid molecular motion in the gel phase using 1-palmitoyl-2-9-(2-anthryl)-nonanoyl-sn-glycero-3-phosphocholine as probe. *Eur. J. Biochem.* 150:341–347.
3. de Bony, J., and J. F. Tocanne. 1984. Photo-induced dimerization of anthracene-phospholipids for the study of the lateral distribution of lipids in membranes. *Eur. J. Biochem.* 143:373–379.
4. Welby, M., and J. F. Tocanne. 1982. Evidence for the incorporation of a fluorescent anthracene fatty acid into the membrane lipids of Micrococcus luteus. *Biochim. Biophys. Acta.* 689:173–176.
5. de Bony, J., G. Martin, M. Welby, and J. F. Tocanne. 1984. Evidence for a homogeneous lateral distribution of lipids in a bacterial membrane. *FEBS (Fed. Eur. Biochem. Soc.)* Lett. 174:1–6.
6. Dupou, L., J. Teissié, and J. F. Tocanne. 1986. Metabolic incorporation of 9-(2-anthryl)-nonanoic acid, a new fluorescent and photoactivable probe, into the membrane lipids of Chinese hamster ovary cells. *Eur. J. Biochem.* 154:171–177.
7. Elson, E. L., and D. Magde. 1974. Fluorescence correlation spectroscopy. I. Conceptual basis and theory. *Biopolymers.* 13:1–27.
8. Axelrod, D., D. E. Koppel, J. Schlessinger, E. Elson, and W. W. Webb. 1976. Mobility measurement by analysis of fluorescence photobleaching recovery kinetics. *Biophys. J.* 16:1055–1069.
9. Soumpasis, D. M. 1983. Theoretical analysis of fluorescence photobleaching recovery experiments. *Biophys. J.* 41:95–97.
10. Lardner, T. J. 1977. The measurement of cell membrane diffusion coefficients. *J. Biomech.* 10:167–170.
11. Teissié, J., J. F. Tocanne, and A. Baudras. 1978. A fluorescence approach of the determination of translational diffusion coefficients of lipids in phospholipid monolayer at the air-water interface. *Eur. J. Biochem.*83:77–85.
12. Wu E., K. Jacobson, and D. Papahadjopoulos. 1977. Lateral diffusion in phospholipid multibilayers measured by fluorescence recovery after photobleaching. *Biochemistry.* 16:3936–3942.
13. Koppel, D. E., D. Axelrod, J. Schlessinger, E. L. Elson, and W. W. Webb. 1976. Dynamics of fluorescent marker concentration as a probe of mobility. *Biophys. J.* 16:1315–1329.
14. Petersen, N. O., and W. B. McConnaughev. 1981. Effects of multiple membranes on measurements of cell surface dynamics by fluorescence photobleaching. *J. Supramol. Struct. Cell. Biochem.* 17:213–221.
15. Peters, R., A. Brunger, and K. Schulten. 1981. Continuous fluorescence microphotolysis: a sensitive method for study of diffusion processes in single cells. *Proc. Natl. Acad. Sci. USA.* 78:962–966.
16. Vaz, W. L. C., Z. I. Derzko, and K. A. Jacobson. 1982. Photobleaching measurements of the lateral diffusion of lipids and proteins in artificial phospholipid bilayer membranes. *Cell Surf. Rev.* 8:83–135.
17. Dupou, L., L. Gualandris, A. Lopez, A. M. Duprat, and J. F. Tocanne. 1987. Alterations in lateral lipid mobility in the plasma membrane of Urodelean ectodermal cells during gastrulation. *Exp. Cell Res.* 169:502–513.
18. de Laat, S. W., P. T. Van der Saag, E. L. Elson, and J. Schlessinger. 1980. Lateral diffusion of membrane lipids and proteins during the cell cycle of neuroblastoma cells. *Proc. Natl. Acad. Sci. USA.* 77:1526–1528.
19. Powell, M. J. D. 1964. New algorithm for minimization process. *Comput. J.* 7:155–161.
20. Lopez, A., F. Loussayre, R. Martino, and A. Lattes. 1985. Etude du phénomène d'autoempilement par densimétrie. *Nouveau J. Chimie.* 9:267–271.
21. Brunger, A., R. Peters, and K. Schulten. 1985. Continuous fluorescence microphotolysis to observe lateral diffusion in membranes. Theoretical methods and applications. *J. Chem. Phys.* 82:2147–2160.
22. Crouzeix, M., and A. H. Mignot. 1983. Analyse Numérique des Equations Différentielles. Masson, Paris.